CEAS Aeronautical Journal (2024) 15:397–408
https://doi.org/10.1007/s13272-023-00701-x

ORIGINAL PAPER

$\mathcal{L}_1$ adaptive fault-tolerant control of stratospheric airships

Toufik Souanef[1] · James Whidborne[1] · Shi Qian Liu[2]

Received: 20 April 2023 / Revised: 15 August 2023 / Accepted: 8 November 2023 / Published online: 26 March 2024
© The Author(s) 2024

Abstract
As the utilization of stratospheric airships becomes more prevalent, ensuring their safe operation becomes crucial. This paper explores the ability of an $\mathcal{L}_1$ adaptive controller to maintain fault tolerance in the actuators of a stratospheric airship. $\mathcal{L}_1$ adaptive control offers fast adaptation while separating adaptation and robustness. This makes the approach a suitable candidate for fault-tolerant control. The performance of the proposed design is compared to the Linear Quadratic Integral and Adaptive Sliding Mode Backstepping controllers. Simulation results show that the robustness of the airship model against faults is improved with the use of the $\mathcal{L}_1$ adaptive controller.

Keywords Adaptive control · Fault-tolerant control · Airship control

1 Introduction

Stratospheric airships, similar to other types of unmanned aerial vehicles, have a range of potential uses for both military and civilian purposes, such as serving as platforms for observation, remote sensing, and communication relay. However, the dynamics of airships are fundamentally nonlinear and different from those of traditional aircraft. Typically, the center of gravity of an airship is located below the center of volume, making it susceptible to changes in air pressure and temperature. In addition, the mass and inertia of the airship are not constant. What is more, airships are generally considered underactuated vehicles, largely due to the lack of a lateral force actuator to counteract aerodynamic side forces, limited roll moments, and limited control surface effectiveness at low airspeeds [1, 2]. Therefore, designing flight control systems for stratospheric airships is a challenging task [3].

For the problem of airship control, many methodologies have been proposed in the literature, such as PID [4, 5], state feedback [6], backstepping control [7], dynamic inversion [8], adaptive control [9], and sliding mode control [10–12]. More details can be found in [13] and references therein.

In common with all aeronautical systems, stratospheric airships faults and failures may have serious consequences. Given the low temperatures and high levels of radiation in the stratosphere, both sensor and actuator failures are likely to occur, thus deteriorating the control performance and even jeopardizing the whole mission. Therefore, more in-depth research is required in this area.

Fault-tolerant control is a control system that can automatically adapt and compensate for failures [14]. Fault-tolerant control systems are categorized as either passive or active [15, 16]. Passive fault-tolerant control is based on robust control and assumes the worst-case conditions [17, 18]. Active fault-tolerant controllers consist of a fault detection mechanism and a supervision module. Based on the information provided by the fault detection module, the supervision module can make decisions on how to reconfigure the controller [19]. A compromise between the two approaches is adaptive control, which is based on the reconfiguration of the controller parameters without involving an explicit fault detection module [20, 21].

Very few approaches have addressed airship fault-tolerant control [13]. In [22], the authors proposed a strong track filter-based method for fault detection and applied it to

Toufik Souanef, James Whidborne and Shi Qian Liu have contributed equally to this work.

✉ Toufik Souanef
toufik.souanef@cranfield.ac.uk

James Whidborne
j.f.whidborne@cranfield.ac.uk

Shi Qian Liu
liushiqian@sjtu.edu.cn

[1] School of Aerospace, Transport and Manufacturing, Cranfield University, College Road, Cranfield, UK

[2] School of Aeronautics and Astronautics, Shanghai Jiao Tong University, Shanghai, China

design a fault-tolerant backstepping attitude control system for autonomous airships in the event of sensor failures. In [23], an adaptive backstepping approach for fault-tolerant attitude control of stratospheric airships with input saturation was presented. Another adaptive integral sliding mode approach has been applied to fault-tolerant tracking control for a multi-vectored thrust ellipsoidal airship in [24]. A fault-tolerant control method based on a constrained adaptive backstepping approach and utilizing a radial basis function neural network approximation was proposed in [25] for airships with thruster faults. The work of [26] dealt with the problem of trajectory tracking for a stratospheric airship in the presence of actuator faults, full-state constraints, input saturation, and unknown external disturbances. A fault-tolerant controller based on an adaptive neural network backstepping approach was proposed to solve this problem. The attitude tracking control of a flexible airship subjected to wind disturbances, actuator saturation, and control surface faults has been studied in [27]. An adaptive fault estimator was designed to estimate the faults of the control surfaces. The common issue of these works is that the backstepping controller is always combined with other techniques to improve its robustness, which might make practical application and tuning relatively complicated. In [28], a fault-tolerant Model Reference Adaptive Control (MRAC) approach for an actuator fault airship model was designed. However, accommodating faults needs to ensure whole stability and uniform boundedness of the system during the transient regime. This is the main drawback of MRAC [29].

$\mathcal{L}_1$ adaptive control is a compelling option for airship fault-tolerant control because of its ability to fast and robust adaptation, resulting in the desired transient performance for both input and output signals [30]. The development of $\mathcal{L}_1$ adaptive control was driven by the need for a more cost-effective validation and verification process for adaptive flight-critical systems [31]. This control method has been utilized in a variety of flight control systems, such as [32–35] to name a few. However, it appears it has not previously been applied to airship control.

Hence, this paper presents the design of an $\mathcal{L}_1$ adaptive fault-tolerant controller for a stratospheric airship. The main advantage is that fast and robust adaptation permits the accommodating of faults and failures and enhances the safety of operation of stratospheric airships. Another advantage is its relative simplicity of implementation compared to the previous methods based on the combination of robust control techniques.

In Sect. 2, the airship model is recalled. Section 3 describes the $\mathcal{L}_1$ adaptive controller design. In Sect. 4, $\mathcal{L}_1$ adaptive control is summarized. Simulations were performed for the airship when subjected to actuator faults, some of the results are presented in Sect. 5, and the results for the controllers are compared. Finally, some conclusions are drawn.

1.1 Notations

Boldface for matrices, vectors, and tensors; italics for all variables and lowercase Greek letters; and roman for all numerals, uppercase Greek characters, and mathematical operators.

$\|\cdot\|_1$ denotes the 1-norm of a vector.

For a stable proper transfer matrix $G(s)$, $\|G(s)\|_{\mathcal{L}_1}$ denotes its $\mathcal{L}_1$-norm. For time-varying signals, we use both time-domain and frequency-domain notations. For example, for the signal $\xi(t)$, defined on $t \in [0, \infty)$, we use $\xi(s)$ for its Laplace transform.

2 Airship model

The stratospheric airship presented in this paper has an ellipsoidal envelope. Buoyancy force is provided by helium contained in the envelope.

The yaw control system consists of the up and down rudder which move in unison. The pitch and roll control systems are composed of the left and right elevators which move separately. The airship is equipped with propellers fixed on both sides of the gondola, which are vector thrust systems that can rotate about their horizontal axis. These propellers provide the primary propulsion for the airship.

The mathematical model of the airship is defined from [36–39]. The kinematic model of the airship is derived by the frames from Fig. 1 [40] and it is formulated as

$$\dot{\Xi}_1(t) = \mathbf{T}\Xi_2(t)$$

where $\Xi_1 = \begin{bmatrix}\boldsymbol{\zeta}^T & \boldsymbol{\eta}^T\end{bmatrix}^T$, $\Xi_2 = \begin{bmatrix}v_a^T & \Omega^T\end{bmatrix}^T$, $\boldsymbol{\zeta} = \begin{bmatrix}x & y & z\end{bmatrix}^T$ is the airship position in the inertial frame, $\boldsymbol{\eta} = \begin{bmatrix}\phi & \theta & \psi\end{bmatrix}^T$ is the attitude vector, $v_a = \begin{bmatrix}u & v & w\end{bmatrix}^T$ and $\Omega = \begin{bmatrix}p & q & r\end{bmatrix}^T$ are the speeds and angular rates in the body frame, respectively, and

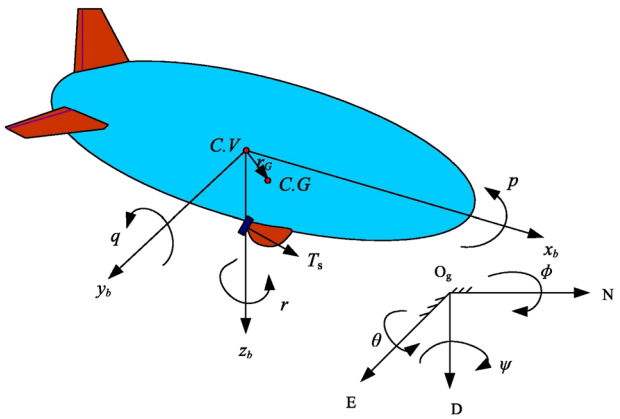

Fig. 1 Airship structure and frames

$$\mathbf{T} = \begin{bmatrix} \mathbf{R}(\boldsymbol{\eta}) & 0 \\ 0 & \mathbf{J}(\boldsymbol{\eta}) \end{bmatrix}$$

where $\mathbf{R}(\boldsymbol{\eta})$ is the direction cosine matrix and $\mathbf{J}(\boldsymbol{\eta})$ is the transformation matrix [40].

The dynamic model of the ariship is given by

$$\mathbf{M}_a \begin{bmatrix} \dot{\mathbf{v}}_a(t) \\ \dot{\Omega}(t) \end{bmatrix} = \begin{bmatrix} \mathbf{F}_k + \mathbf{F}_w + \mathbf{F}_{GB} + \mathbf{F}_A \\ \mathbf{N}_k + \mathbf{N}_w + \mathbf{N}_{GB} + \mathbf{N}_A \end{bmatrix} + \begin{bmatrix} \mathbf{F} \\ \mathbf{N} \end{bmatrix}, \tag{1}$$

where $\mathbf{M}_a$ represents the generalized mass matrix, $\mathbf{F}_k$ represents the kinetics force vector, $\mathbf{F}_w$ represents the wind-induced force vector, $\mathbf{F}_{GB}$ represents the sum of the gravity and buoyancy vectors, $\mathbf{F}_A$ denotes the aerodynamic force vector, $\mathbf{F}$ represents the control input and thrust vector, $\mathbf{N}_k, \mathbf{N}_w, \mathbf{N}_{GB}, \mathbf{N}_A$, and $\mathbf{N}$ are associated moments generated by $\mathbf{F}_k, \mathbf{F}_w, \mathbf{F}_{GB}, \mathbf{F}_A$, and $\mathbf{F}$, respectively.

Let

$$\mathbf{U} = \begin{bmatrix} \mathbf{F} \\ \mathbf{N} \end{bmatrix}, \tag{2}$$

then (1) can be rewritten as

$$\dot{\Xi}_2(t) = \mathbf{f}_2 + \mathbf{g}_2 \mathbf{U}(t), \tag{3}$$

where

$$\mathbf{f}_2 = \mathbf{M}_a^{-1} \cdot \begin{bmatrix} \mathbf{F}_k + \mathbf{F}_w + \mathbf{F}_{GB} + \mathbf{F}_A \\ \mathbf{N}_k + \mathbf{N}_w + \mathbf{N}_{GB} + \mathbf{N}_A \end{bmatrix}$$
$$\mathbf{g}_2(\Xi) = \mathbf{M}_a^{-1}$$

Given that the airship is underactuated in the y-direction, or lacks an effector to counteract aerodynamic side forces [1], then Eq. (2) can be rewritten as follows

$$\begin{bmatrix} f_x \\ f_z \\ n_x \\ n_y \\ n_z \end{bmatrix} = \begin{bmatrix} 1 & 0 & 0 & 0 & 0 & 0 \\ 0 & 1 & \bar{q}C_{z\delta_e} & \bar{q}C_{z\delta_e} & 0 & 0 \\ 0 & 0 & \bar{q}C_{l\delta_e} & -\bar{q}C_{l\delta_e} & \bar{q}C_{l\delta_r} & -\bar{q}C_{l\delta_r} \\ dz & dx & \bar{q}C_{m\delta_e} & \bar{q}C_{m\delta_e} & 0 & 0 \\ 0 & 0 & 0 & 0 & \bar{q}C_{n\delta_r} & \bar{q}C_{n\delta_r} \end{bmatrix} \begin{bmatrix} T_x \\ T_z \\ \delta_{eL} \\ \delta_{eR} \\ \delta_{rU} \\ \delta_{rB} \end{bmatrix}, \tag{4}$$

where $C_{z\delta_e}, C_{l\delta_e}, C_{l\delta_r}, C_{m\delta_e}, C_{n\delta_r}$ are the aerodynamic coefficients of the control surfaces, T_x and T_z are the thrust components in the x_b and z_b axis, respectively. d_x and d_z represent the distance from the CV to the propeller in the x_b and z_b axis.

The thrusts can be linearized by the following transformation [1]

$$\begin{cases} T_x = (T_p + T_s)\cos\mu \\ T_z = -(T_p + T_s)\sin\mu \end{cases} \tag{5}$$

where T_p and T_s represent the thrusts of the port and starboard side, respectively. The tilting angle can be computed as $\mu = \mathrm{atan}(-T_z/T_x)$, with maximum and minimum values of 90° and −90°, respectively.

A traditional approach in flight control is to control separately the inner-loop and the outer-loop. The outer-loop (trajectory) vector is $\boldsymbol{\zeta}$. The inner-loop (body frame velocity, rotation rates and attitude) vector is $\bar{\mathbf{x}} = [\Xi_2,\ \boldsymbol{\eta}] = [u,\ v,\ w,\ p,\ q,\ r,\ \phi,\ \theta,\ \psi]$.

The objective of this paper is to compute the the input $\mathbf{U} = [f_x, f_z, n_x, n_y, n_z]$ of desired forces and moments so that the inner-loop follows the reference input from the trajectory controller.

Remark 1 It is obvious that airship aerodynamic and mass uncertainties, external disturbances, potential faults and/or failures can degrade the control system performance and even cause instability if they are not explicitly addressed in control design.

3 $\mathcal{L}_1$ adaptive controller design

Given the model in (2), and considering external disturbances as a vector $\boldsymbol{\mu}(t)$, the attitude dynamics of the airship can be written in a compact form as

$$\dot{\bar{\mathbf{x}}}(t) = \mathbf{f}(\bar{\mathbf{x}}) + \mathbf{g}(\bar{\mathbf{x}})\mathbf{U}(t) + \boldsymbol{\mu}(t). \tag{6}$$

A typical approach in designing adaptive control is to linearize the non-linear model around a specific equilibrium or operating point. Hence, a linear controller can be developed based on the linearized system model and then by adding the adaptive controller, it allows for improved robustness of the system. Actually, it permits for less "burden" of the adaptive controller through the use of prior knowledge of the system [41].

As for all aeronautical systems, the airship is in trim flight when the net forces and moments sum to zero. This includes contributions from the aerodynamics, gravity, buoyancy, and thrust [42].

By linearization about a trim (equilibrium) point, the non-linear system in (6) can be approximated by

$$\dot{\mathbf{x}}(t) = \mathbf{A}_p \mathbf{x}(t) + \mathbf{B}_p \mathbf{u}(t) + \tilde{\boldsymbol{\mu}}(\mathbf{x}, \mathbf{u}, t), \tag{7}$$

where $\bar{\mathbf{x}}(t) = \mathbf{x}_0(t) + \mathbf{x}(t)$, where $\mathbf{x}_0(t)$ represents the trim vector, $\mathbf{U}(t) = \mathbf{u}_0(t) + \mathbf{u}(t)$, $\mathbf{u}_0(t)$ is the trim command, $\tilde{\boldsymbol{\mu}}(\mathbf{x}, \mathbf{u}, t)$ is a non-linear unknown function that includes the higher order terms of the Taylor series expansion of $\mathbf{f}(\mathbf{x}) + \mathbf{g}(\mathbf{x})\mathbf{U}$, $\boldsymbol{\mu}(t)$ and the external disturbance, $\mathbf{A}_p \in \mathbb{R}^{9\times9}$ and $\mathbf{B}_p \in \mathbb{R}^{9\times5}$ are unknown matrices

Remark 2 As a result of the system linearization, as it is common in the control of aeronautical systems, two

decoupled movements can be considered, namely longitudinal and lateral:

- The longitudinal motion consists of the states $\mathbf{x}_{lon} = [u\ w\ q\ \theta]$ and the inputs $\mathbf{u}_{lon} = [f_x f_z\ n_y]$.
- The lateral motion consists of the states $\mathbf{x}_{lat} = [v\ p\ r\ \phi\ \psi]$ and the inputs $\mathbf{u}_{lat} = [n_x\ n_z]$.

Separate controllers are developed for each mode as shown in Fig. 2.

3.1 Longitudinal controller design

Considering only the longitudinal state vector $\mathbf{x}_{lon}$ and the longitudinal input $\mathbf{u}_{lon}$, the reduced system from (7) can be written as

$$\dot{\mathbf{x}}_{lon}(t) = \mathbf{A}_{lon}\mathbf{x}_{lon}(t) + \mathbf{B}_{lon}\mathbf{u}_{lon}(t) + \tilde{\mathbf{f}}_{lon}(t), \tag{8}$$

where $\mathbf{A}_{lon} \in \mathbb{R}^{4\times4}$ is the uncertain matrix of the longitudinal dynamics, $\mathbf{B}_{lon} \in \mathbb{R}^{4\times3}$ is the uncertain matrix of longitudinal inputs and $\tilde{\mathbf{f}}_{lon} \in \mathbb{R}^4$ is an unknown function. The output is $y_{lon} = [u\ q\ \theta]$.

Since the matrices $\mathbf{A}_{lon}$ and $\mathbf{B}_{lon}$ are unknown, the following approximations can be made:

$$\mathbf{A}_{lon} = \mathbf{A}_1 + \Delta\mathbf{A}_{lon}, \tag{9}$$

where $\mathbf{A}_1 \in \mathbb{R}^{4\times4}$ is a known matrix estimated assuming nominal conditions and parameters, $\Delta\mathbf{A} \in \mathbb{R}^{4\times4}$ is an unknown matrix of the system dynamics, and

$$\mathbf{B}_{lon} = \mathbf{B}_1(\mathbb{I}_3 + \Delta\mathbf{B}_1),, \tag{10}$$

where $\mathbf{B}_1 \in \mathbb{R}^{4\times3}$ is a known matrix, $\Delta\mathbf{B}_1 \in \mathbb{R}^{3\times3}$ is an unknown matrix of the control input uncertainties.

By neglecting the unknown parameters, the nominal system can be written from (8) as

$$\dot{\mathbf{x}}_{lon}(t) = \mathbf{A}_1\mathbf{x}_{lon}(t) + \mathbf{B}_1\mathbf{u}_{lon}(t), \tag{11}$$

Next, an LQR controller is designed for the system with nominal parameters defined in (11). Recalling the LQR controller from [43], for the following linear system

$$\dot{\mathbf{x}}(t) = \mathbf{A}\,\mathbf{x}(t) + \mathbf{B}\,\mathbf{u}(t), \tag{12}$$

as the control law $\mathbf{u}(t) = -\mathbf{K}\mathbf{x}(t)$ that minimizes the quadratic cost function

$$J = \int_0^\infty \left(\mathbf{x}^T\mathbf{Q}\mathbf{x}(t) + \mathbf{u}^T(t)\mathbf{R}\mathbf{u}(t)\right)dt \tag{13}$$

where $\mathbf{Q}$ and $\mathbf{R}$ are weighting matrices, with

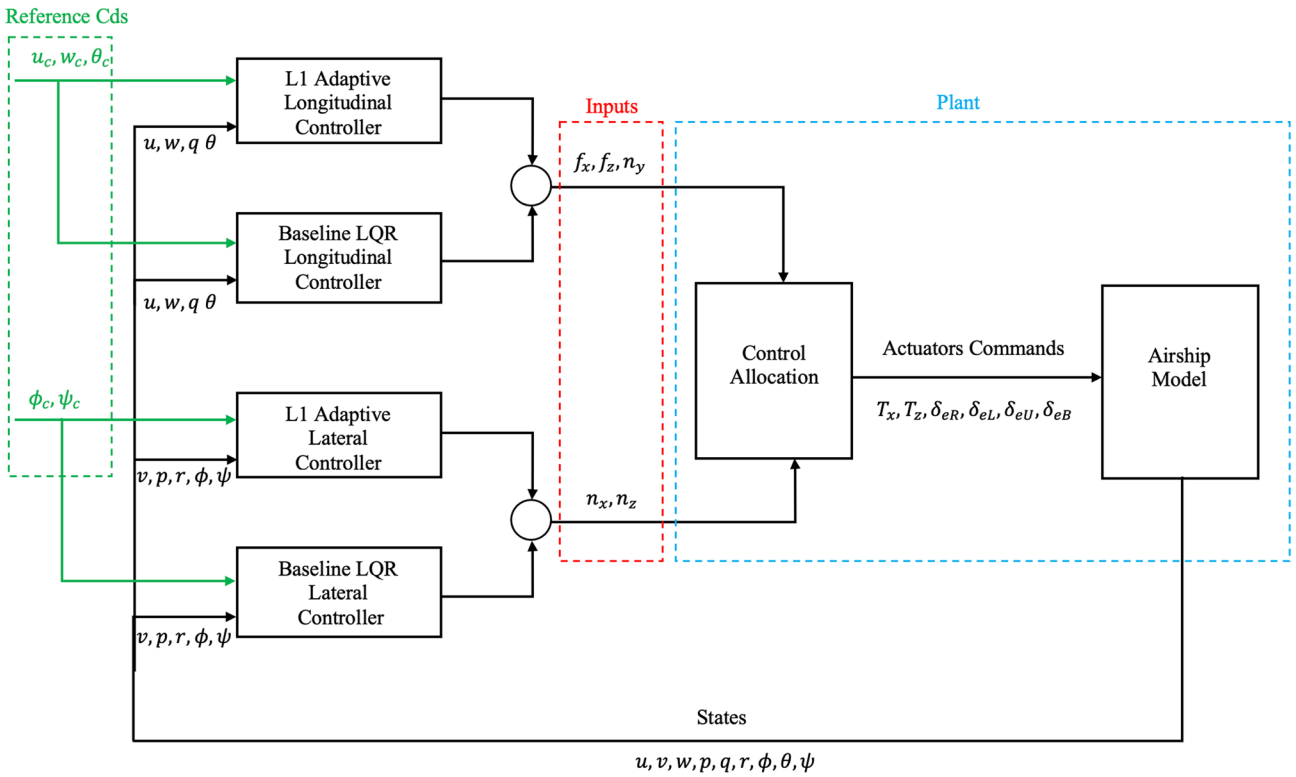

Fig. 2 Control architecture

$$\mathbf{K} = \mathbf{R}^{-1}\mathbf{B}^T\mathbf{P} \tag{14}$$

where $\mathbf{P} = \mathbf{P}^T \geq 0$ is the solution to

$$\mathbf{A}^T\mathbf{P} + \mathbf{P}\mathbf{A} + \mathbf{Q} - \mathbf{P}\mathbf{B}\,\mathbf{R}^{-1}\mathbf{B}^T\mathbf{P} = 0. \tag{15}$$

Hence, the control law $\mathbf{u}_{lon}$ for the system in (8) can be written as follows

$$\mathbf{u}_{lon} = -\mathbf{k}_{p_1}^{\top}\bar{\mathbf{x}}_1 + \mathbf{u}_1, \tag{16}$$

where $\mathbf{k}_{p_1}$ is the feedback matrix of the LQR controller and $\mathbf{u}_1$ is the adaptive control law that compensates for unknown disturbances and system parameters. The choice of the feedback gain $\mathbf{k}_{p_1}$ is a gain matrix that defines $\mathbf{A}_{m1} = \mathbf{A}_1 + \mathbf{B}_1\mathbf{k}_{p_1}$, where $\mathbf{A}_{m1} \in \mathbb{R}^{4\times4}$ is a Hurwitz matrix that defines the desired dynamics of the system.

The system that is ultimately controlled by the adaptive control is as follows

$$\dot{\mathbf{x}}_1(t) = \mathbf{A}_{m_1}\mathbf{x}_1(t) + \mathbf{B}_1\boldsymbol{\omega}_1\mathbf{u}_1(t) + \tilde{\mathbf{h}}_1(t,\mathbf{x}), \tag{17}$$

where $\boldsymbol{\omega}_1 = \mathbb{I}_3 + \Delta\mathbf{B}_1$ and $\tilde{\mathbf{h}}_1(t,x) = \Delta\mathbf{A}_1\mathbf{x}(t) + (\boldsymbol{\omega}_1 - \mathbb{I}_3)K_1\mathbf{x}_1(t) + \tilde{\mathbf{f}}_1$.

Assuming $\tilde{\mathbf{h}}_1(t,\mathbf{x}) = \mathbf{B}_1\left(\boldsymbol{\theta}_1\mathbf{x}_1(t) + \boldsymbol{\sigma}_{m_1}(t)\right) + \mathbf{B}_{u_1}\sigma_{u_1}(t)$, the system in (17) can be parametrized as follows

$$\dot{\mathbf{x}}_1(t) = \mathbf{A}_{m_1}\mathbf{x}(t) + \mathbf{B}_1\left(\boldsymbol{\omega}_1\mathbf{u}_1(t) + \boldsymbol{\theta}_1\mathbf{x}_1(t) + \boldsymbol{\sigma}_{m_1}(t)\right) + \mathbf{B}_{u_1}\sigma_{u_1}(t), \tag{18}$$

where $\boldsymbol{\theta}_1$ is a matrix of constant unknown parameters representing model uncertainties, with dimension $\mathbb{R}^{3\times4}$, $\sigma_{m_1}(t)$ is an unknown matched disturbance of dimension $\mathbb{R}^3$, $\sigma_{u_1}(t)$ is an unknown unmatched scalar disturbance, and $\mathbf{B}_{u_1}$ is a constant matrix of dimension $\mathbb{R}^{4\times1}$ such that $\mathbf{B}_1^T\mathbf{B}_{u_1} = 0$ and the matrix $\left[\mathbf{B}_1;\mathbf{B}_{u_1}\right]$ has rank 4.

3.2 Lateral controller design

The design of the lateral controller is similar to the longitudinal controller. Considering only the lateral state vector $\mathbf{x}_{lat}$ and the lateral input $\mathbf{u}_{lat}$, the reduced system from (7) can be written as

$$\dot{\mathbf{x}}_{lat}(t) = \mathbf{A}_{lat}\mathbf{x}_{lat}(t) + \mathbf{B}_{lat}\mathbf{u}_{lat}(t) + \tilde{\mathbf{f}}_{lat}(t), \tag{19}$$

where $\mathbf{A}_{lat} \in \mathbb{R}^{5\times5}$ is an unknown matrix of the lateral dynamics, $\mathbf{B}_{lat} \in \mathbb{R}^{5\times2}$ is an unknown matrix of lateral inputs, and $\tilde{\mathbf{f}}_{lat} \in \mathbb{R}^5$ is an unknown function. The output is $\mathbf{y}_{lat} = [\phi\ \psi]$.

Similarly to the longitudinal dynamics, the system with nominal parameters can be written as follows

$$\dot{\mathbf{x}}_{lat}(t) = \mathbf{A}_2\mathbf{x}_{lat}(t) + \mathbf{B}_2\mathbf{u}_{lat}(t), \tag{20}$$

Proceeding in a similar way as Eqs. (16) to (17) leads to the following model for the lateral system

$$\dot{\mathbf{x}}_2(t) = \mathbf{A}_{m_2}\mathbf{x}_2(t) + \mathbf{B}_2\left(\boldsymbol{\omega}_2\mathbf{u}_2(t) + \boldsymbol{\theta}_2\mathbf{x}_2(t) + \boldsymbol{\sigma}_{m_2}(t)\right) + \mathbf{B}_{u_2}\sigma_{u_2}(t,x), \tag{21}$$

where $\boldsymbol{\theta}_2$ is a matrix of constant unknown parameters representing model uncertainties, with dimension $\mathbb{R}^{2\times5}$, $\boldsymbol{\sigma}_{m_2}(t)$ is an unknown matched disturbance of dimension $\mathbb{R}^2$, $\boldsymbol{\sigma}_{u_2}(t)$ is an unknown unmatched disturbance of dimension $\mathbb{R}^{2\times2}$, and $\mathbf{B}_{u_2}$ is a constant matrix of dimension $\mathbb{R}^{5\times2}$ such that $\mathbf{B}_1^T\mathbf{B}_{u_1} = 0$ and the matrix $\left[\mathbf{B}_1;\mathbf{B}_{u_1}\right]$ has rank 4.

The objective is to design control inputs $\mathbf{u}_1(t)$ and $\mathbf{u}_2(t)$ that would make the chosen system outputs track reference commands with bounded errors in the presence of uncertainties external disturbances.

The resulting models in (18) and (21) make straightforward application of $\mathcal{L}_1$ adaptive control that is described in the next section.

4 $\mathcal{L}_1$ adaptive control

Both airship longitudinal and lateral control formulations in (18) and (21) are equivalent to the general class of systems defined by

$$\begin{aligned}\dot{\mathbf{x}}(t) &= \mathbf{A}_m\mathbf{x}(t) + \mathbf{B}\left(\boldsymbol{\omega}\mathbf{u}(t) + \boldsymbol{\theta}\mathbf{x}(t) + \boldsymbol{\sigma}_m(t)\right) + \mathbf{B}_u\boldsymbol{\sigma}_u(t,\mathbf{x}),\\ \mathbf{y}(t) &= \mathbf{C}\mathbf{x}(t),\end{aligned} \tag{22}$$

where $\mathbf{A}_m = \in \mathbb{R}^{n\times n}$ is the matrix of the desired system dynamics, $\mathbf{B} \in \mathbb{R}^{n\times m}$ is a known matrix, $\mathbf{C} \in \mathbb{R}^{m\times n}$ is a known matrix, $\mathbf{x}(t) \in \mathbb{R}^n$ is the state vector which is assumed to be available through measurement, $\mathbf{u}(t) \in \mathbb{R}^m$ is the control input vector, $\boldsymbol{\theta}^{\top} \in \mathbb{R}^{m\times n}$ is a matrix of constant unknown parameters representing model uncertainties, $\boldsymbol{\sigma}_m(t) \in \mathbb{R}^m$ is an unknown matched disturbance, $\boldsymbol{\sigma}_u(t) \in \mathbb{R}^n$ is an unknown unmatched disturbance, $\mathbf{B}_u \in \mathbb{R}^{n\times(n-m)}$ is a constant matrix such that $\mathbf{B}^T\mathbf{B}_u = 0$, $\left[\mathbf{B}\ \mathbf{B}_{um}\right]$ has rank n.

Assumption 1 The unknown model parameters are restricted within a known compact convex set Θ, represented by $\boldsymbol{\theta} \in \Theta$. The system input gain matrix $\boldsymbol{\omega}$ is assumed to be an unknown (non-singular) strictly row-diagonally dominant matrix with the sign of ω_{ii} known. It is also assumed that there exists a known compact convex set Ω, such that $\boldsymbol{\omega} \in \Omega \subset \mathbb{R}^{m\times m}$. The disturbances $\boldsymbol{\sigma}_m(t)$ and $\boldsymbol{\sigma}_u(t)$ are restricted within known compact sets Δ_m and Δ_u, respectively. In addition, it is assumed that both disturbances are differentiable with bounded derivatives, meaning there exist finite reals d_{σ_m} and d_{σ_u} such that:

$$\|\dot{\boldsymbol{\sigma}}_m(t)\|_2 \leq d_{\sigma_m}, \quad \|\dot{\boldsymbol{\sigma}}_u(t)\|_2 \leq d_{\sigma_u} \quad \forall t \geq 0.$$

Remark 3 These assumptions, from a practical point of view, are indeed reasonable. They are based on conservative knowledge about the magnitude of airship uncertainties obtained through analysis, experimental evaluation, or wind-tunnel testing. For instance, assuming known maximum possible variations of aerodynamic coefficients concerning nominal values is entirely justifiable. Such assumptions align with conventions for real-world systems, where technical specifications or engineering insights usually establish known compact ranges for unknown parameters that the system can accommodate without any compromise.

The architecture of the $\mathcal{L}_1$ adaptive controller is made up of three components: a state predictor, an adaptation law, and a control law, as shown in Fig. 3.

The state prediction is determined by

$$\dot{\hat{\mathbf{x}}}(t) = \mathbf{A}_m\hat{\mathbf{x}}(t) + \mathbf{B}\big(\hat{\boldsymbol{\omega}}(t)\mathbf{u}(t) + \hat{\boldsymbol{\theta}}(t)\mathbf{x}(t) + \hat{\boldsymbol{\sigma}}_m(t)\big) + \mathbf{B}_u\hat{\boldsymbol{\sigma}}_u(t), \tag{23}$$

where $\hat{\omega}(t)$, $\hat{\boldsymbol{\theta}}(t)$, $\hat{\boldsymbol{\sigma}}_m(t)$, and $\hat{\boldsymbol{\sigma}}_u(t)$ are the estimates of the unknown system parameters and $\hat{\mathbf{x}}(t)$ is the estimate of the state vector $\mathbf{x}(t)$.

The adaptation laws are defined as

$$\begin{aligned}
\dot{\hat{\boldsymbol{\omega}}} &= \Gamma\ \ \mathrm{Proj}\big(\hat{\boldsymbol{\omega}}, -(\tilde{\mathbf{x}}^\top \P\mathbf{B})^\top\mathbf{u}^\top\big),\\
\dot{\hat{\boldsymbol{\theta}}} &= \Gamma\ \ \mathrm{Proj}\big(\hat{\boldsymbol{\theta}}, -(\tilde{\mathbf{x}}^\top \P\mathbf{B})^\top\mathbf{x}^\top\big),\\
\dot{\hat{\boldsymbol{\sigma}}}_m(t) &= \Gamma\ \ \mathrm{Proj}\big(\hat{\sigma}_m, -(\tilde{\mathbf{x}}^\top \P\mathbf{B})^\top\big),\\
\dot{\hat{\boldsymbol{\sigma}}}_u(t) &= \Gamma\ \ \mathrm{Proj}\big(\hat{\sigma}_u, -(\tilde{\mathbf{x}}^\top \P\mathbf{B}_u)^\top\big),
\end{aligned} \tag{24}$$

where $\tilde{\mathbf{x}} = \hat{\mathbf{x}} - \mathbf{x}$ is the prediction error, $\Gamma > 0$ is the adaptation gain, and $\mathbb{P}$ is the solution of the algebraic Lyapunov equation $(\mathbf{A}_m)^\top\P + \P\mathbf{A}_m = -\mathbf{Q}$, $\mathbf{Q} > 0$, while $\mathrm{Proj}(\cdot,\cdot)$ denotes the projection operator defined over the sets Θ, Ω, Δ_m, and Δ_u (more details in the appendix).

Remark 4 The adaptation law is based on Lyapunov stability theory and ensures that the prediction error remains bounded. As a result, this guarantees assured transient performance for the $\mathcal{L}_1$ adaptive controller. Further details can be found in [30, 44].

Let

$$\begin{aligned}
\mathbf{H}_m(s) &= \mathbf{C}\big(s\mathbb{I} - \mathbf{A}_m\big)^{-1}\mathbf{B},\\
\mathbf{H}_0(s) &= \mathbf{C}\big(s\mathbb{I} - \mathbf{A}_m\big)^{-1}.
\end{aligned} \tag{25}$$

The control law is given by

$$\mathbf{u}(s) = \mathbf{K}\,\mathbf{F}(s)\Big(\mathbf{K}_g\, r(s) - \hat{v}(s)\Big), \tag{26}$$

where $\hat{v}(s) = \hat{v}_1(s) + \hat{v}_2(s)\hat{\sigma}_u(s)$, $\hat{v}_1(s)$ is the Laplace transform of $\hat{v}_1(t) = \hat{\omega}(t)\mathbf{u}(t) + \hat{\sigma}_m(t)$, $\hat{v}_2(s) = \mathbf{H}_m^{-1}(s)\mathbf{H}_0(s)\hat{\sigma}_u(s)$, $\mathbf{K}_g = -(\mathbf{C}\mathbf{A}_m^{-1}\mathbf{B})^{-1}$ is a pre-filter of the MIMO control law, $\mathbf{F}(s)$ is an $m \times m$ strictly proper transfer matrix and $\mathbf{K} \in \mathbb{R}^{m\times m}$.

For analysis purposes, without loss of generality, $\mathbf{F}(s)$ is chosen as $\mathbf{F}(s) = \frac{\mathbf{D}(s)}{s}$, where $\mathbf{D}(s)$ is a proper stable transfer function. Hence, the control law can be written:

$$\mathbf{u}(s) = K\,\frac{\mathbf{D}(s)}{s}\Big(\mathbf{K}_g\,\mathbf{r}(s) - \hat{\boldsymbol{\nu}}(s)\Big), \tag{27}$$

which leads, for all $\boldsymbol{\omega} \in \Omega$, to a strictly proper stable

$$\mathbf{G}(s) \triangleq \boldsymbol{\omega}\mathbf{K}\mathbf{D}(s)\big(s\mathbb{I}_m + \boldsymbol{\omega}\mathbf{K}\mathbf{D}(s)\big)^{-1}, \tag{28}$$

with DC gain $\mathbf{G}(0) = \mathbb{I}_m$.

The $\mathcal{L}_1$ adaptive controller is subjected to the $\mathcal{L}_1$ norm condition [30]

$$\|\bar{\mathbf{G}}(s)\|_{\mathcal{L}_1} L < 1 \tag{29}$$

where $L = \max_{\theta\in\Theta}\|\boldsymbol{\theta}\|_{\mathcal{L}_1} = \max_i\Big(\sum_j\big|\theta_{ij}\big|\Big)$ and $\bar{\mathbf{G}}(s) = \big(s\mathbb{I} - A_m\big)^{-1}\mathbf{B}(\mathbb{I} - \mathbf{G}(s))$.

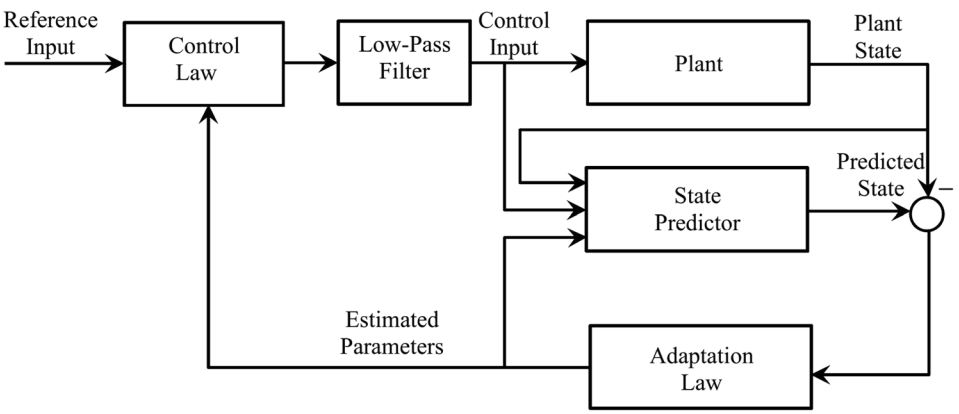

Fig. 3 Block diagram of the $\mathcal{L}_1$ adaptive controller

In addition, the selection of $\mathbf{D}(s)$ must guarantee that $\mathbf{G}(s)\mathbf{H}_m^{-1}(s)$ is a properly stable transfer matrix.

Remark 5 Controller analysis is straightforward from [30] and [44], and is omitted here.

5 Simulation for airship fault-tolerant control

The objective of the simulations is to evaluate the performance of the $\mathcal{L}_1$ adaptive controller for airship attitude control, compared to the Adaptive Sliding Mode Backstepping (ASMB) controller proposed in [39] and the Linear Quadratic Integral (LQI) controller.

In this context, robustness refers to the controller ability to keep attitude errors within an acceptable range despite varying disturbances and uncertainties.

The evaluation is based on the observation of the system output and analyzing how the $\mathcal{L}_1$ adaptive controller performs, in comparison with the LQI and ASMB controllers. The main goal is to determine how the system response with the $\mathcal{L}_1$ adaptive controller is smoother and more accurate compared to the responses of the LQI and ASMB controllers.

5.1 Airship LQI control

The design of the LQI controller is first outlined, with a focus on improving robustness against disturbances in the longitudinal controller. To achieve this, we incorporate the integral of the regulated output error, represented by $\mathbf{e}_{lon}(t) = \int_0^t \mathbf{r}_{lon}(t) - \mathbf{y}_{lon}(t)$, into the linear system in (11). $\mathbf{r}_{lon}$ is the desired output for the longitudinal controller.

The augmented system can be written as follows

$$\underbrace{\begin{bmatrix}\dot{\mathbf{x}}_{lon}\\ \dot{\mathbf{e}}_{lon}\end{bmatrix}}_{\dot{\mathbf{x}}_1} = \underbrace{\begin{bmatrix}\mathbf{A}_1 & 0\\ -\mathbf{C}_{lon} & 0\end{bmatrix}}_{\bar{\mathbf{A}}_1}\underbrace{\begin{bmatrix}\mathbf{x}_{lon}\\ \mathbf{e}_{lon}\end{bmatrix}}_{\mathbf{x}_1} + \underbrace{\begin{bmatrix}\mathbf{B}_1\\ 0_{3\times 3}\end{bmatrix}}_{\bar{\mathbf{B}}_1}\mathbf{u}_{lon} + \underbrace{\begin{bmatrix}0_{4\times 3}\\ \mathbb{I}_3\end{bmatrix}}_{\mathbf{B}_{l_1}}\mathbf{r}_{lon}. \tag{30}$$

The control law for the longitudinal system is defined as follows

$$\mathbf{u}_{lon} = -\mathbf{k}_{p_1}^{\top}\bar{\mathbf{x}}_1 - \mathbf{k}_{i_1}^{\top}\mathbf{e}_{lon}, \tag{31}$$

where the proportional feedback gain vector $\mathbf{k}_{p_1}^{\top}$ is designed to achieve the same system dynamics matrix as the $\mathcal{L}_1$ adaptive controller $\mathbf{A}_{m_1} = \mathbf{A}_1 - \mathbf{B}_1\,\mathbf{k}_{p_1}^{\top}$ and $\mathbf{k}_{i_1}$ is the integral gain vector of the LQI controller.

The design of the lateral controller is similar to the longitudinal controller. We consider for the system in (19) the integral of the regulated output error, denoted by

$$\mathbf{e}_{lat}(t) = \int_0^t \mathbf{r}_{lat}(t) - \mathbf{y}_{lat}(t),$$

where $\mathbf{r}_{lat}$ is the commanded output for the lateral controller.

The augmented system of (20) can be written as follows

$$\underbrace{\begin{bmatrix}\dot{\mathbf{x}}_{lat}\\ \dot{\mathbf{e}}_{lat}\end{bmatrix}}_{\dot{\mathbf{x}}_1} = \underbrace{\begin{bmatrix}\mathbf{A}_2 & 0\\ -\mathbf{C}_{lat} & 0\end{bmatrix}}_{\bar{\mathbf{A}}_1}\underbrace{\begin{bmatrix}\mathbf{x}_{lat}\\ \mathbf{e}_{lat}\end{bmatrix}}_{\mathbf{x}_1} + \underbrace{\begin{bmatrix}\mathbf{B}_2\\ 0_{3\times 3}\end{bmatrix}}_{\bar{\mathbf{B}}_1}\mathbf{u}_{lat} + \underbrace{\begin{bmatrix}0_{4\times 3}\\ \mathbb{I}_2\end{bmatrix}}_{\mathbf{B}_{l_1}}\mathbf{r}_{lat}. \tag{32}$$

The control law for the lateral system is defined as follows

$$\mathbf{u}_{lat} = -\mathbf{k}_{p_2}^{\top}\bar{\mathbf{x}}_2 - \mathbf{k}_{i_2}^{\top}\mathbf{e}_{lat}, \tag{33}$$

where the proportional feedback gain vector $\mathbf{k}_{p_2}^{\top}$ is designed to achieve the same system dynamics matrix as the $\mathcal{L}_1$ adaptive controller $\mathbf{A}_{m_2} = \mathbf{A}_2 - \mathbf{B}_2\,\mathbf{k}_{p_2}^{\top}$ and $\mathbf{k}_{i_2}$ is the integral gain vector of the LQI controller.

5.2 Simulation results

The considered model is a 250 m length, 75 m diameter airship [42]. For the design of the $\mathcal{L}_1$ adaptive controller, the transfer functions $\mathbf{D}_{1,2}(s) = \frac{1}{s(s+9.8)}$ and $k = 36$. The design of the $\mathcal{L}_1$ adaptive controller aims for robustness against model uncertainties within specified ranges. These ranges include $\omega_{1,2} = [0.25,\ 1.75]$, $\Delta_{1,2} = 10$ and $\Theta_{1,2} = \{\theta_i \in [-2\ 2], i = 1, 9\}$. The ASMB controller gains are chosen as in [39] with similar dynamics to the LQI and the $\mathcal{L}_1$ adaptive controllers.

To achieve this goal, the controllers were evaluated under three different scenarios to determine their performance: without failures, with elevator failure, and with rudder failure. The root mean square of the tracking error (RMSE) was used as a performance evaluation metric for the controllers.

In all cases, a time-varying wind disturbance with components given by $[0, 5 + 5\sin(2\pi t), 5 + 5\sin(2\pi t)]^{\top}$ m/s, was introduced at a simulation time of t = 60 s.

5.2.1 Nominal case

In the nominal case, no failures were introduced in the system, except the time-varying wind disturbance at simulation time t = 60 *s*.

Simulation results indicate that all controllers perform well in the absence of wind disturbances, as demonstrated

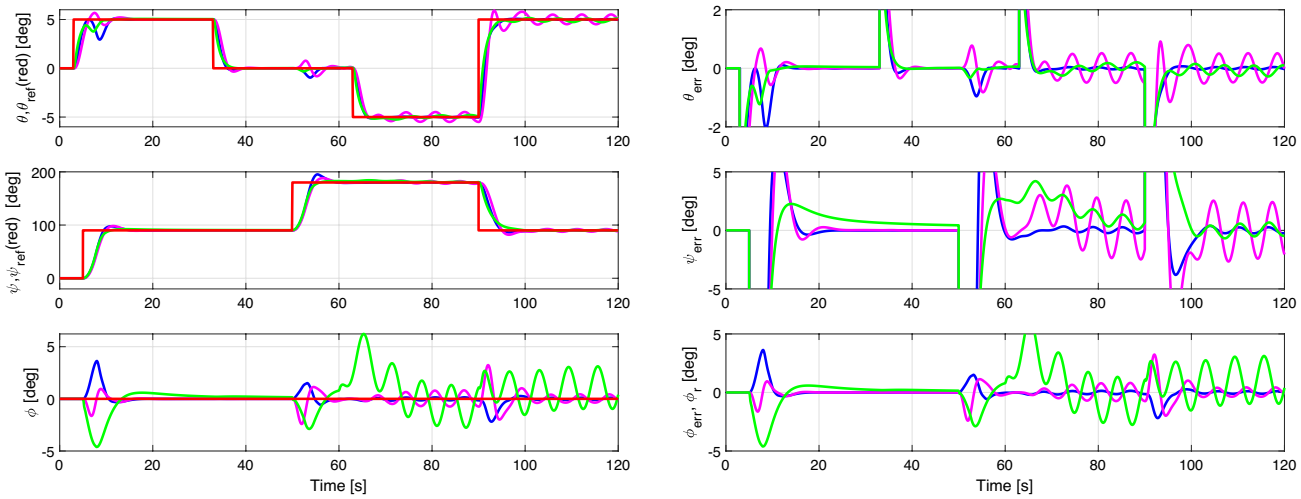

(a) Attitude angles vs References. (b) Attitude errors.

Fig. 4 Attitude angles for nominal case with wind inputs ($\mathcal{L}_1$ blue, LQI magenta, ASMB green)

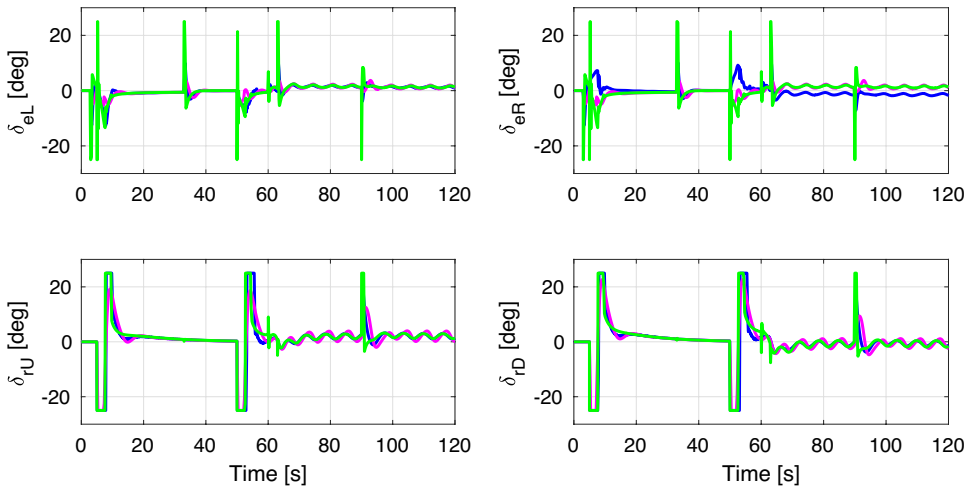

Fig. 5 Rudder and elevator commands for nominal case with wind inputs ($\mathcal{L}_1$ blue, LQI magenta, ASMB green)

by the attitude angles of the airship relative to desired references in Fig. 4. The performance of the three controllers is similar before the introduction of wind disturbances and the commands are within acceptable limits, as illustrated in Fig. 5.

When the wind disturbance was introduced, it became clear that for the lateral-directional system, the $\mathcal{L}_1$ adaptive controller performed better than both the ASMB and LQRI controllers. This difference is evident in Fig. 4, where it can be observed that the amplitude of attitude errors is larger with the ASMB and LQRI controllers, especially in the case of the roll angle. The roll angle, in particular, cannot be directly compensated for because the airship lacks ailerons. For the pitch angle, the ASMB controller performs better than the $\mathcal{L}_1$ adaptive controller, as shown in Table 1.

Table 1 RMSE analysis in the nominal case

Angle	Controller	RMSE Total	RMSE Before disturbance	RMSE After disturbance
Pitch θ	$\mathcal{L}_1$	1.25	0.99	1.46
	ASMB	1.03	0.81	1.21
	LQR	1.47	1.11	1.76
Roll ϕ	$\mathcal{L}_1$	0.56	0.68	0.41
	ASMB	1.70	1.23	2.07
	LQR	0.60	0.49	0.69
Yaw ψ	$\mathcal{L}_1$	20.25	24.18	15.34
	ASMB	19.48	23.69	14.05
	LQR	21.68	24.91	17.87

However, as can be observed in Fig. 5, this performance of the ASMB controller is attributed to impulses in the elevator command when using the ASMB controller. In practical applications, this may be a serious issue, as it can burden the actuators and cause them to operate beyond their nominal range. Similar impulses with relatively low amplitude can also be observed in the rudder command.

It should be noted that attempts to mitigate these impulses and achieve a smoother command response were unsuccessful without compromising the ASMB controller response time and overall performance.

5.2.2 Pitch control under failure of the elevator command

Elevator command failure in an airship significantly impacts pitch control, limiting altitude stability and maneuverability, potentially compromising safety and operational efficiency.

To evaluate the controller performance under elevator command faults, the following scenario was considered:

- Complete loss of effectiveness (100%) of the left elevator command δ_{eL} at simulation time t = 20 s;
- Constant bias in the right elevator command δ_{eR} at simulation time t = 30 s;
- Time-varying wind disturbance with components x, y and z-directions given by $[5, 5 + 5\sin(2\pi t, 5 + 5\sin(2\pi t)]^{\top}$ m/s at simulation time t = 60 s.

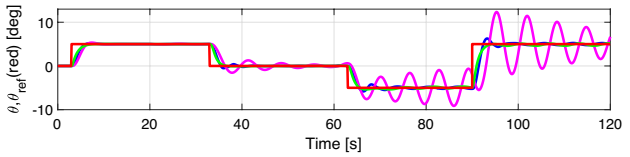

(a) Pitch angles vs Reference.

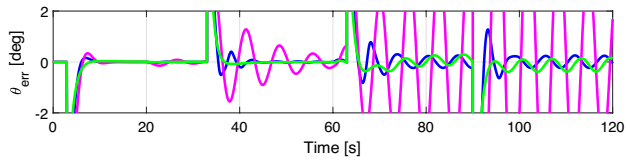

(b) Pitch errors.

Fig. 6 Pitch angle for elevator failure case with wind inputs ($\mathcal{L}_1$ blue, LQI magenta, ASMB green)

Table 2 Pitch angle RMSE analysis in the nominal case

Angle	Controller	RMSE Total	RMSE Before disturbance	RMSE After disturbance
Pitch θ	$\mathcal{L}_1$	1.28	0.96	1.54
	ASMB	1.06	0.86	1.25
	LQR	2.79	1.21	3.76

The goal was to replicate failure scenarios that the system could encounter during real-world operation.

The pitch angle of the airship relative to the desired reference is illustrated in Fig. 6. The RMSE analysis of the pitch angle response to the desired reference in Table 2 shows that the $\mathcal{L}_1$ adaptive controller outperforms the LQI controller in the case of elevator failure under wind conditions. However, in this scenario, the ASMB controller demonstrates better performance than the $\mathcal{L}_1$ adaptive controller.

Nevertheless, similar to the nominal case, as it is shown in Fig. 7, it becomes evident that the elevator command with the $\mathcal{L}_1$ adaptive controller is smoother compared to the ASMB controller, and it does not manifest the elevator command spikes observed in the case of the ASMB controller

These simulations conclude that the $\mathcal{L}_1$ adaptive controller demonstrates relatively better performance over the ASMB and LQI controllers in the presence of elevator failures.

5.2.3 Lateral/directional control under failure of the rudder command

The goal was to evaluate the system performance in case of failure of the rudder command.

The rudder plays a crucial role in controlling the yaw motion of the airship, which is essential for maintaining stability and directional control. Without the ability to control yaw through the rudder, the airship's ability to change its heading or direction could be severely compromised. This could lead to difficulties in navigating, turning, and maintaining a desired course, potentially affecting the overall control and safety of the airship during flight.

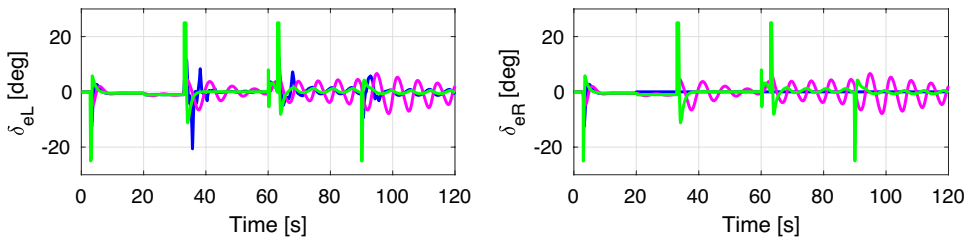

Fig. 7 Elevator commands for failure case with wind inputs ($\mathcal{L}_1$ blue, LQI magenta, ASMB green)

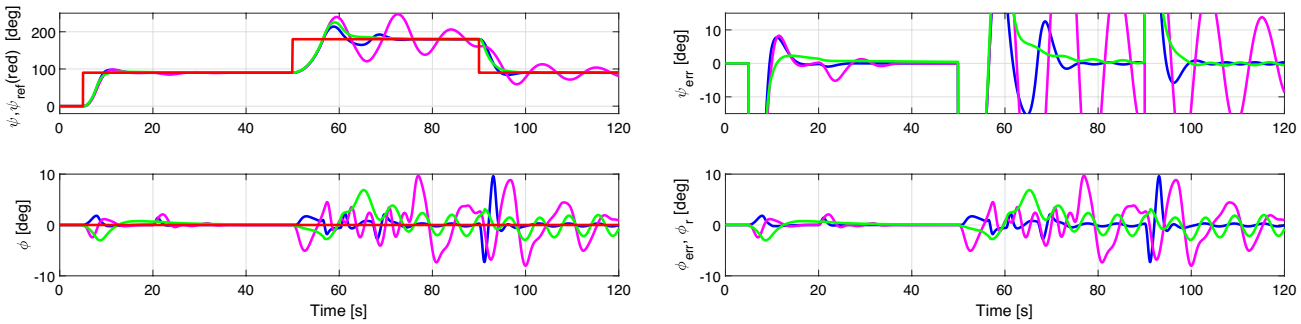

(a) Attitude angles vs References. (b) Attitude errors.

Fig. 8 Attitude angles for rudder failure case with wind inputs ($\mathcal{L}_1$ blue, LQI magenta, ASMB green)

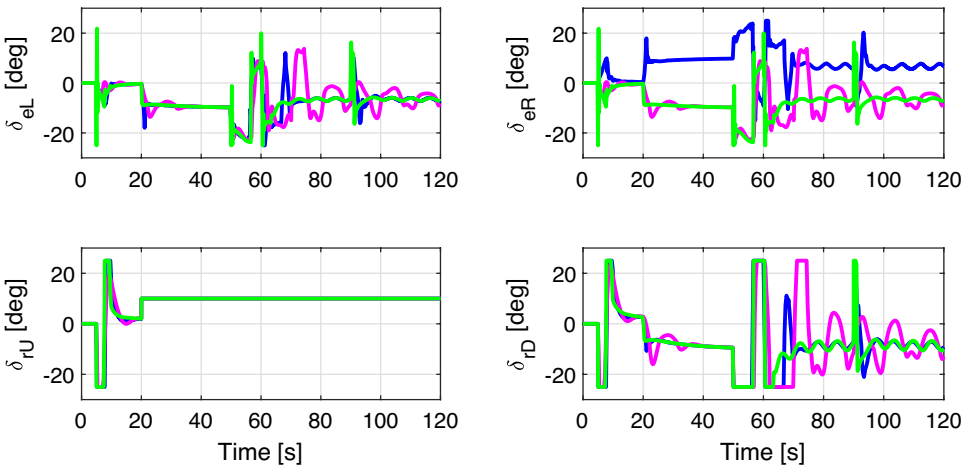

Fig. 9 Rudder and elevator commands for rudder failure case with wind inputs ($\mathcal{L}_1$ blue, LQI magenta, ASMB green)

To replicate this situation, the following scenario was considered:

- Lock in place at position 10 deg of the upper rudder command δ_{rU} at simulation time t = 20 s;
- Time-varying wind disturbance with components x, y and z-directions given by $[5, 5 + 5\sin(2\pi t, 5 + 5\sin(2\pi t)]^\top$m/s at simulation time t = 60 s.

The lateral/directional angles of the airship relative to the desired references are illustrated in Fig. 8. The $\mathcal{L}_1$ adaptive controller performs better than the ASMB and the LQI controller in the case of rudder lock-in-place in wind conditions. This is especially true for roll angle control. From Fig. 9, it appears that with the $\mathcal{L}_1$ adaptive controller, the right elevator command δ_{eR} permits to produce the necessary roll command to counteract the effect of the bias of the rudder, which reflects the good performance of the controller in controlling the roll angle ϕ. This is confirmed by the RMSE analysis of the roll and yaw outputs to the references, as shown in Table 3. As expected, the LQI controller has shown the worst performance.

Table 3 RMSE analysis in the nominal case

Angle	Controller	RMSE Total	RMSE Before disturbance	RMSE After disturbance
Roll ϕ	$\mathcal{L}_1$	1.16	0.63	1.54
	ASMB	1.70	0.84	2.222
	LQR	2.91	1.62	3.91
Yaw ψ	$\mathcal{L}_1$	23.44	32.74	16.45
	ASMB	19.48	33.42	15.29
	LQR	30.90	34.91	31.44

6 Conclusion

This paper presents an approach for $\mathcal{L}_1$ adaptive fault-tolerant control of stratospheric airships. The adaptive controller shows better performance in simulations compared to Linear Quadratic Integral (LQI) and Adaptive Sliding Mode Backstepping (ASMB) controllers. This is especially true for attitude control in the presence of failures and external disturbances.

Thus, the advantages of the $\mathcal{L}_1$ adaptive controller are evident. This approach can potentially be applied to other airship systems, for instance, airships controlled using moving mass technologies [45]. Another research direction is the integrated guidance and control of airships in stratospheric winds.

Practical validation is the ultimate goal to showcase the effectiveness of the proposed design. However, performing direct physical tests on a full-scale stratospheric airship is a complex, challenging, and expensive task due to factors such as the high altitudes at which these airships operate, the specialized equipment required, safety coordination, operating procedures limitations, and the associated costs.

Appendix: the projection operator

The projection-type adaptive law permits to maintain the unknown parameters within their predefined sets [46].

Due to their inherent time-variant and non-linear behavior, adaptive controllers cannot be certified via the metrics used for linear conventional controllers, such as gain and phase margin. Projection operator is a robustness augmentation technique that bounds the output of a non-linear adaptive controller while conforming to the Lyapunov stability rules. It can also be used to limit the control authority of the adaptive component so that the said control authority can be arbitrarily close to that of a linear controller [47].

The projection operator is defined for two vectors $f, p \in \mathbb{R}^n$ by

$$\text{proj}(\mathbf{p}, \mathbf{z}) := \begin{cases} \mathbf{z} & \text{if } f(\mathbf{p}) < 0, \\ \mathbf{z} & \text{if } f(\mathbf{p}) \geqslant 0 \text{ and } \nabla f(\mathbf{p})^T \mathbf{z} \leqslant 0, \\ \mathbf{z} - \frac{(\nabla f)^T \mathbf{z}}{\|\nabla f\|^2} \nabla f f & \text{if } f(\mathbf{p}) \geqslant 0 \text{ and } \nabla f(\mathbf{p})^T \mathbf{z} > 0, \end{cases}$$

where $f : \mathbb{R}^n \to \mathbb{R}$ is a smooth, convex function given by:

$$f(\mathbf{p}) = \frac{(\varepsilon_p + 1)\mathbf{p}^T \mathbf{p} - p_{\max}^2}{\varepsilon_p p_{\max}^2}$$

where $p_{\max}$ is a norm bound imposed on the vector $\mathbf{p}$, and $\varepsilon_p > 0$ is a chosen tolerance bound.

Data availability The data that support the findings of this study are available from the corresponding author toufik.souanef@cranfield.ac.uk, upon reasonable request.

Declarations

Consent to participate All of the authors declare the consent to participate in this manuscript.

Consent for publication All of the authors declare the consent to publish this manuscript.

Conflict of interest There is no conflict of interest or competing interest.

Ethics approval This paper does not contain research that requires ethical approval.

Open Access This article is licensed under a Creative Commons Attribution 4.0 International License, which permits use, sharing, adaptation, distribution and reproduction in any medium or format, as long as you give appropriate credit to the original author(s) and the source, provide a link to the Creative Commons licence, and indicate if changes were made. The images or other third party material in this article are included in the article's Creative Commons licence, unless indicated otherwise in a credit line to the material. If material is not included in the article's Creative Commons licence and your intended use is not permitted by statutory regulation or exceeds the permitted use, you will need to obtain permission directly from the copyright holder. To view a copy of this licence, visit http://creativecommons.org/licenses/by/4.0/.

References

1. Azinheira, J.R., Moutinho, A., De Paiva, E.C.: Airship hover stabilization using a backstepping control approach. J. Guid. Control. Dyn. **29**(4), 903–914 (2006)
2. Azinheira, J.R., Moutinho, A., de Paiva, E.C.: A backstepping controller for path-tracking of an underactuated autonomous airship. Int. J. Robust Nonlinear Control **19**(4), 418–441 (2009)
3. Gomes, S.B.V., Ramos, J.G.: Airship dynamic modeling for autonomous operation. In: Proceedings. 1998 IEEE International Conference on Robotics and Automation, vol. 4, pp. 3462–3467 (1998). ICRA
4. de Paiva, E.C., Bueno, S.S., Gomes, S.B., Ramos, J.J., Bergerman, M.: A control system development environment for aurora's semi-autonomous robotic airship. In: Proceedings 1999 IEEE International Conference on Robotics and Automation, vol. 3, pp. 2328–2335 (1999). ICRA
5. Azinheira, J.R., de Paiva, E.C., Ramos, J., Beuno, S.: Mission path following for an autonomous unmanned airship. In: Proceedings 2000 ICRA. Millennium Conference. IEEE International Conference on Robotics and Automation, vol. 2, pp. 1269–1275 (2000). ICRA
6. Hygounenc, E., Soueres, P.: Lateral path following gps-based control of a small-size unmanned blimp. In: 2003 IEEE International Conference on Robotics and Automation (Cat. No. 03CH37422), vol. 1, pp. 540–545 (2003). IEEE
7. Beji, L., Abichou, A.: Tracking control of trim trajectories of a blimp for ascent and descent flight manoeuvres. Int. J. Control **78**(10), 706–719 (2005)
8. Moutinho, A., Azinheira, J.R.: Stability and robustness analysis of the Aurora airship control system using dynamic inversion.

In: Proceedings of the 2005 IEEE International Conference on Robotics and Automation, pp. 2265–2270 (2005). ICRA
9. Yan, Z., Weidong, Q., Yugeng, X., Zili, C.: Stabilization and trajectory tracking of autonomous airship's planar motion. J. Syst. Eng. Electron. **19**(5), 974–981 (2008)
10. Wang, X.L., Liu, D., Shan, X.X.: Study on the three dimensional trajectory control for airship. J. Shanghai Jiaotong Univ. (Chin. Ed.) **40**(12), 2164 (2006)
11. Paiva, E., Benjovengo, F., Bueno, S., Ferreira, P.: Sliding mode control approaches for an autonomous unmanned airship. In: 18th AIAA Lighter-Than-Air Systems Technology Conference, p. 2869 (2009)
12. Yang, Y.N., Wu, J., Zheng, W.: Trajectory tracking for an autonomous airship using fuzzy adaptive sliding mode control. J. Zhejiang Univ. Sci. **13**(7), 534–543 (2012)
13. Zuo, Z., Song, J., Zheng, Z., Han, Q.-L.: A survey on modelling, control and challenges of stratospheric airships. Control. Eng. Pract. **119**, 104979 (2022)
14. Zhang, Y., Jiang, J.: Bibliographical review on reconfigurable fault-tolerant control systems. Annu. Rev. Control. **32**(2), 229–252 (2008)
15. Hwang, I., Kim, S., Kim, Y., Seah, C.E.: A survey of fault detection, isolation, and reconfiguration methods. IEEE Trans. Control Syst. Technol. **18**(3), 636–653 (2009)
16. Rotondo, D.: Advances in Gain-scheduling and Fault-tolerant Control Techniques. Springer, Cham (2017)
17. Edwards, C., Spurgeon, S.K., Akoachere, A.: A sliding mode static output feedback controller based on linear matrix inequalities applied to an aircraft system. J. Dyn. Syst. Meas. Contr. **122**, 656 (2000)
18. Amin, A.A., Hasan, K.M.: A review of fault tolerant control systems: advancements and applications. Measurement **143**, 58–68 (2019)
19. Abbaspour, A., Mokhtari, S., Sargolzaei, A., Yen, K.K.: A survey on active fault-tolerant control systems. Electronics **9**(9), 1513 (2020)
20. Tao, G.: Adaptive Control of Systems with Actuator Failures. Springer, London (2004)
21. Ma, Y., Jiang, B., Tao, G., Badihi, H.: Minimum-eigenvalue-based fault-tolerant adaptive dynamic control for spacecraft. J. Guid. Control. Dyn. **43**(9), 1764–1771 (2020)
22. Wu, G., Lin, B., Zhang, S.: Fault-tolerant backstepping attitude control for autonomous airship with sensor failure. Procedia Engineering **29**, 2022–2027 (2012)
23. Liang, Z., Zheng, Z., Zhu, M., Wu, Z.: Adaptive fault tolerant attitude control of a stratospheric airship with input saturation. In: 13th IEEE International Conference on Control & Automation (ICCA), pp. 443–448 (2017)
24. Xiao, C., Han, D., Wang, Y., Zhou, P., Duan, D.: Fault-tolerant tracking control for a multi-vectored thrust ellipsoidal airship using adaptive integral sliding mode approach. Proceedings of the Institution of Mechanical Engineers, Part G: Journal of Aerospace Engineering **232**(10), 1911–1924 (2018)
25. Liu, S., Whidborne, J.F.: Neural network adaptive backstepping fault tolerant control for unmanned airships with multi-vectored thrusters. Proceedings of the Institution of Mechanical Engineers, Part G: Journal of Aerospace Engineering **235**(11), 1507–1520 (2021)
26. Gou, H., Zhu, M., Zheng, Z., Guo, X., Lou, W., Yuan, J.: Adaptive fault-tolerant control for stratospheric airships with full-state constraints, input saturation, and external disturbances. Adv. Space Res. **69**(1), 701–717 (2022)
27. Liu, S., Whidborne, J.F., Song, S., Lyu, W.: Adaptive backstepping nonsingular terminal sliding-mode attitude control of flexible airships with actuator faults. Aerospace **9**(4), 209 (2022)
28. Joshi, H., Sinha, N.K.: Adaptive fault tolerant control design for stratospheric airship with actuator faults. IFAC-PapersOnLine **55**(1), 819–825 (2022)
29. Wise, K.A., Lavretsky, E., Hovakimyan, N.: Adaptive control of flight: theory, applications, and open problems. In: 2006 American Control Conference, p. 6 (2006)
30. Hovakimyan, N., Cao, C.: L_1 Adaptive Control Theory: Guaranteed Robustness with Fast Adaptation, vol. 21. Siam, Philedelphia (2010)
31. Hovakimyan, N., Cao, C., Kharisov, E., Xargay, E., Gregory, I.M.: L_1 adaptive control for safety-critical systems. IEEE Control. Syst. **31**(5), 54–104 (2011)
32. Dobrokhodov, V., Xargay, E., Hovakimyan, N., Kaminer, I., Cao, C., Gregory, I.M.: Multicriteria analysis of an L_1 adaptive flight control system. Proceedings of the Institution of Mechanical Engineers, Part I: Journal of Systems and Control Engineering **227**(4), 413–427 (2013)
33. Xu, D., Whidborne, J.F., Cooke, A.: Fault tolerant control of a quadrotor using L_1 adaptive control. International. Journal of Intelligent Unmanned Systems **4**(1), 43–66 (2016). https://doi.org/10.1108/IJIUS-08-2015-0011
34. Zhou, Y., Liu, H., Guo, H., Duan, X.: L_1 adaptive dynamic inversion attitude control for unmanned aerial vehicle with actuator failures. Proceedings of the Institution of Mechanical Engineers, Part G: Journal of Aerospace Engineering **233**(11), 4129–4140 (2019)
35. Souanef, T.: Adaptive Guidance and Control of Small Unmanned Aerial Vehicles. Shaker Verlag, Germany (2019)
36. Gomes, S.: An investigation into the flight dynamics of airships with application to the YEZ-2A. PhD thesis, Cranfield University (1990)
37. Moutinho, A., Azinheira, J.R., de Paiva, E.C., Bueno, S.S.: Airship robust path-tracking: A tutorial on airship modelling and gain-scheduling control design. Control. Eng. Pract. **50**, 22–36 (2016)
38. Li, Y., Nahon, M., Sharf, I.: Airship dynamics modeling: A literature review. Prog. Aerosp. Sci. **47**(3), 217–239 (2011)
39. Liu, S.Q., Sang, Y.J., Whidborne, J.F.: Adaptive sliding-mode-backstepping trajectory tracking control of underactuated airships. Aerosp. Sci. Technol. **97**, 105610 (2020)
40. Liu, S.Q., Whidborne, J.F., He, L.: Backstepping sliding-mode control of stratospheric airships using disturbance-observer. Adv. Space Res. **67**(3), 1174–1187 (2021)
41. Lavretsky, E., Wise, K.A.: Robust Adaptive Control, pp. 317–353. Springer, London (2013)
42. Mueller, J., Paluszek, M., Zhao, Y.: Development of an aerodynamic model and control law design for a high altitude airship. In: AIAA 3rd" Unmanned Unlimited" Technical Conference, Workshop and Exhibit, p. 6479 (2004)
43. Stevens, B.L., Lewis, F.L., Johnson, E.N.: Aircraft Control and Simulation: Dynamics, Controls Design, and Autonomous Systems. John Wiley, New Jersey (2015)
44. Cao, C., Hovakimyan, N.: L_1 adaptive controller for multi-input multi-output systems in the presence of unmatched disturbances. In: American Control Conference, 2008, pp. 4105–4110 (2008). IEEE
45. Li, J., Gao, C., Li, C., Jing, W.: A survey on moving mass control technology. Aerosp. Sci. Technol. **82**, 594–606 (2018)
46. Pomet, J.-B., Praly, L., et al.: Adaptive nonlinear regulation: Estimation from the lyapunov equation. IEEE Trans. Autom. Control **37**(6), 729–740 (1992)
47. Larchev, G., Campbell, S., Kaneshige, J.: Projection operator: A step toward certification of adaptive controllers. In: AIAA Infotech@ Aerospace 2010, p. 3366 (2010)

Publisher's Note Springer Nature remains neutral with regard to jurisdictional claims in published maps and institutional affiliations.

https://dspace.org/

L1 adaptive faulttolerant control of stratospheric airships

Souanef, Toufik; Whidborne, James F.; Liu, Shi Qian

2024-04-01
Springer
https://doi.org/10.1007/s13272-023-00701-x
Souanef T, Whidborne J, Liu SQ. (2024) L1 adaptive faulttolerant control of stratospheric airships, CEAS Aeronautical Journal. Volume 15, April 2024, pp. 397-408

Downloaded from a DSpace repository. https://dspace.org/